Conductance modulation of spin interferometers

M. Cahay*
Department of Electrical and Computer Engineering and Computer Science, University of Cincinnati, Cincinnati, Ohio 45221, USA

S. Bandyopadhyay
Department of Electrical Engineering, Virginia Commonwealth University, Richmond, Virginia 23284, USA
(Received 19 March 2003; published 26 September 2003)

We study the conductance modulation of gate controlled electron spin interferometers (also known as spin field effect transistors) based on the Rashba spin–orbit coupling effect. It is found that the modulation is dominated by Ramsauer (or Fabry-Perot) type transmission resonances rather than the Rashba effect in typical structures. These transmission resonances are due to reflections at the interferometer's contacts caused by large interface potential barriers and effective mass mismatch between the contact material and the semiconductor. They are particularly strong in quasi-one-dimensional structures which, in fact, are preferred for spin interferometers because of the energy independence of the spin precession angle. Thus, unless particular care is taken to eliminate Ramsauer resonances by proper contact engineering, any observed conductance modulation of spin interferometers may *not* have its origin in the Rashba effect.

DOI: 10.1103/PhysRevB.68.115316 PACS number(s): 72.25.Dc, 72.25.Mk, 73.21.Hb, 85.35.Ds

I. INTRODUCTION

In a seminal paper, Datta and Das[1] proposed a gate controlled electron spin interferometer consisting of a quasi one-dimensional semiconductor channel with ferromagnetic source and drain contacts (Fig. 1). Electrons are injected with a definite spin from the source, which is controllably precessed in the channel with a gate-controlled Rashba interaction,[2] and finally sensed at the drain. At the drain end, the electron's transmission probability depends on the relative alignment of its spin with the drain's (fixed) magnetization. By controlling the angle of spin precession in the channel with a gate voltage, one can control the relative spin alignment at the drain end, and hence control the source-to-drain current (or conductance).

Despite the immense influence of this device on the field of spintronics, there has never been a complete calculation of the spin interferometer's conductance as a function of the gate voltage in realistic structures. In this paper, we report this calculation and show that there are unsuspected obstacles to the realization of such a device.

II. RAMSAUER EFFECT

In a spin interferometer, varying the gate voltage to precess the spin will also inevitably move the Fermi level up or down relative to the conduction band edge in the interferometer's channel. This causes a different type of conductance modulation. Referring to Fig. 2 (which shows the energy diagram for a spin interferometer), if we neglect the Rashba effect momentarily, then the transmission through the semiconducting channel of the interferometer (barrier region) should peak each time the Fermi level lines up with the resonant energy levels above the barrier between the two contacts.[3] As the gate voltage is varied, the Fermi level sweeps through the resonant levels causing the conductance to oscillate. This is the Ramsauer effect which can become the major source of the conductance modulation of a spin interferometer.

Recently, Matsuyama *et al.*[4] found these oscillations in a *two-dimensional* (2D) spin interferometer. In the 2D case, the oscillations are somewhat muted by ensemble averaging over the transverse wave vector of the electron (and therefore do not completely mask the conductance modulation due to

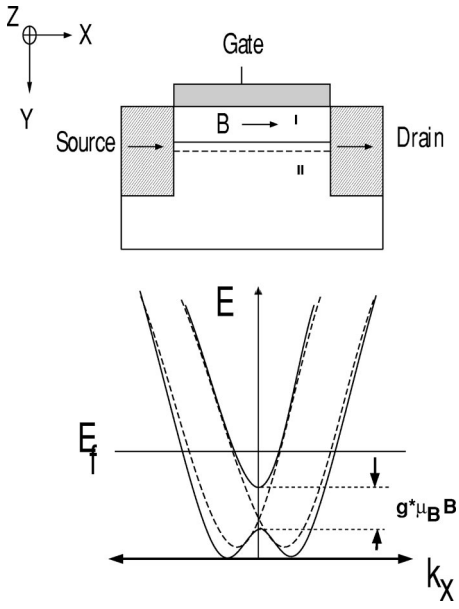

FIG. 1. A schematic of the electron spin interferometer from Ref. 1. The horizontal dashed line represents the quasi-one-dimensional electron gas formed at the semiconductor interface between materials I and II. The magnetization of the ferromagnetic contacts is assumed to be along the $+x$-direction which results in a magnetic field along the x-direction. Also shown is a qualitative representation of the energy dispersion of the two perturbed (solid line) and unperturbed (broken line) bands under the gate. The unperturbed bands are given by Eq. (3) and the perturbed ones are given by Eqs. (4) and (5) in the text.

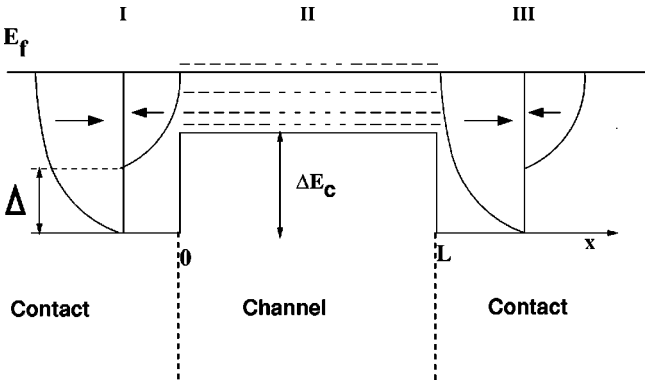

FIG. 2. Energy band diagram across the electron spin interferometer. We use a Stoner-Wohlfarth model for the ferromagnetic contacts. Δ is the exchange splitting energy in the contacts. ΔE_c is the height of the potential barrier between the energy band bottoms of the semiconductor and the ferromagnetic contacts. ΔE_c takes into account the effects of the quantum confinement in the *y*- and *z*-directions. Also shown as dashed lines are the resonant energy states above ΔE_c. Peaks in the conductance of the electron spin interferometer are expected when the Fermi level in the contacts lines up with the resonant states.

the gate controlled spin precession), but in the 1D case which is considered here, the oscillations are much more pronounced because of the lack of ensemble averaging over the transverse wave vector. This presents a quandary for the device designer since a 1D interferometer is preferred over a 2D counterpart from the point of view of energy-independent spin precession.[1] Yet it turns out that the advantage of one-dimensionality may be lost because of the pronounced Ramsauer oscillations.

III. THEORY

The quasi-one-dimensional spin interferometer is described by the single particle effective-mass Hamiltonian,[6]

$$\mathcal{H}=\frac{1}{2m^*}(\boldsymbol{p}+e\boldsymbol{A})^2+V_1(y)+V_2(z)-(g^*/2)\mu_B\boldsymbol{B}\cdot\boldsymbol{\sigma}+\frac{\alpha_R}{\hbar}\hat{y}\cdot[\boldsymbol{\sigma}\times(\boldsymbol{p}+e\boldsymbol{A})], \tag{1}$$

where $\hat{y}$ is the unit vector normal to the heterostructure interface in Fig. 1 and $\boldsymbol{A}$ is the vector potential due to the axial magnetic field $\boldsymbol{B}$ along the channel caused by the ferromagnetic contacts (this magnetic field was summarily ignored in all previous work,[4,7,8] but has important consequences). This field, which is directed along the channel, can be quite strong when the ferromagnetic contacts are magnetized in the same direction. Based on recent work by Wrobel *et al.*,[5] we estimate that this field will be as high as 1 Tesla if the channel length is of the order of 100 nm. The quantity α_R in Eq. (1) is the Rashba coupling strength which varies with the applied potential on the gate. We will assume that the confining potentials along the *y*- and *z*-directions are $V_1(y)$ and $V_2(z)$ with the latter being parabolic and the former could be triangular, parabolic or any other kind. This is synergistic with realistic 1D structures grown by most techniques (V-groove, film growth followed by lithography, etc.).

The choice of the Landau gauge $\boldsymbol{A}=(0,-Bz,0)$ allows us to decouple the *y*-component of the Hamiltonian in (2) from the x–z component. Accordingly, the two-dimensional Hamiltonian in the plane of the channel (x–z plane) is

$$H_{xz}=\frac{p_z^2}{2m^*}+\Delta E_c+\frac{1}{2}m^*(\omega_0^2+\omega_c^2)z^2+\frac{\hbar^2k_x^2}{2m^*}+\frac{\hbar^2k_Rk_x}{m^*}\sigma_z-(g^*/2)\mu_BB\sigma_x-\frac{\hbar k_Rp_z}{m^*}\sigma_x, \tag{2}$$

where ω_0 is the curvature of the confining potential in the *z*-direction, $\omega_c=eB/m^*$, μ_B is the Bohr magneton, g^* is the magnitude of the Landé factor in the channel, $k_R=m^*\alpha_R/\hbar^2$, and ΔE_c is the potential barrier between the ferromagnet and semiconductor. We assume that ΔE_c includes the effects of the quantum confinement in the *y*-direction.

A. Energy dispersion relations

We now derive the energy dispersion relations in the spin interferometer's channel from Eq. (2). The first five terms of the Hamiltonian in Eq. (2) yield shifted parabolic subbands with dispersion relations,

$$E_{n,\uparrow}=(n+1/2)\hbar\omega+\Delta E_c+\frac{\hbar^2k_x^2}{2m^*}+\frac{\hbar^2k_Rk_x}{m^*},$$

$$E_{n,\downarrow}=(n+1/2)\hbar\omega+\Delta E_c+\frac{\hbar^2k_x^2}{2m^*}-\frac{\hbar^2k_Rk_x}{m^*}, \tag{3}$$

where $\omega=\sqrt{\omega_0^2+\omega_c^2}$. In Eq. (3), the $\uparrow$ and $\downarrow$ arrows indicate $+z$ and $-z$ polarized spins (eigenstates of the σ_z operator) which are split by the Rashba effect [fifth term in Eq. (2)]. These subbands have definite spin quantizations axes along $+z$ and $-z$ directions. Their dispersion relations (two horizontally displaced parabolas) are shown as dashed lines in Fig. 1.

The sixth and seventh terms in Eq. (2) induce a mixing between the $+z$- and $-z$-polarized spins. The sixth term originates from the magnetic field due to the ferromagnetic contacts and the seventh originates from the Rashba effect itself. The sixth term was ignored and the seventh was assumed to be negligibly small in Ref. 1. The ratio of the sixth and seventh term can be shown to be of the order of 10^4–10^6 for typical values of the relevant parameters. Therefore, we can neglect the seventh term in comparison with the sixth term.

To obtain an analytical expression for the dispersion relation corresponding to the first six terms in the Hamiltonian in Eq. (2), we derive a two-band dispersion relation in a truncated Hilbert space considering mixing between the two lowest unperturbed subband states (namely the $+z$ and $-z$ spin states). Straightforward diagonalization of the Hamiltonian in Eq. (2) (minus the seventh term) in the basis of these two unperturbed states gives the following dispersion relations for the two bands,

$$E_1(k_x)=\frac{1}{2}\hbar\omega+\Delta E_c+\frac{\hbar^2k_x^2}{2m^*}-\sqrt{\left(\frac{\hbar^2k_Rk_x}{m^*}\right)^2+\left(\frac{g^*\mu_BB}{2}\right)^2}, \quad (4)$$

$$E_2(k_x)=\frac{1}{2}\hbar\omega+\Delta E_c+\frac{\hbar^2k_x^2}{2m^*}+\sqrt{\left(\frac{\hbar^2k_Rk_x}{m^*}\right)^2+\left(\frac{g^*\mu_BB}{2}\right)^2}. \quad (5)$$

These dispersion relations are plotted schematically as solid lines in Fig. 1.

From equations (4) and (5), we find that an electron with energy E has wave vectors in the two bands given by

$$k_{x,1}=\frac{1}{\hbar}\sqrt{2m^*\left(\frac{B+\sqrt{B^2-4C}}{2}\right)},$$

$$k_{x,2}=\frac{1}{\hbar}\sqrt{2m^*\left(\frac{B-\sqrt{B^2-4C}}{2}\right)}, \quad (6)$$

where

$$B=2\left(E-\frac{\hbar\omega}{2}-\Delta E_c\right)+4\delta_R,$$

$$C=\left(E-\frac{\hbar\omega}{2}-\Delta E_c\right)^2-\beta^2, \quad \beta=g^*\mu_BB/2. \quad (7)$$

The eigenspinors for these wave vector states are

$$\begin{bmatrix}C_1(k_{x,1})\\C_1'(k_{x,1})\end{bmatrix}=\begin{bmatrix}-\alpha(k_{x,1})/\gamma(k_{x,1})\\ \beta/\gamma(k_{x,1})\end{bmatrix},$$

$$\begin{bmatrix}C_2(k_{x,2})\\C_2'(k_{x,2})\end{bmatrix}=\begin{bmatrix}\beta/\gamma(k_{x,2})\\ \alpha(k_{x,2})/\gamma(k_{x,2})\end{bmatrix}, \quad (8)$$

where the quantities α and γ are given by

$$\alpha(k_x)=\frac{\hbar^2k_Rk_x}{m^*}+\sqrt{\left(\frac{\hbar^2k_Rk_x}{m^*}\right)^2+\beta^2}, \quad \gamma(k_x)=\sqrt{\alpha^2+\beta^2}. \quad (9)$$

Note that the eigenspinors in Eq. (8) are not $+z$-polarized state $[1\ 0]^\dagger$, or $-z$-polarized state $[0\ 1]^\dagger$ if the magnetic field $B\neq0$ (which makes ($\beta\neq0$). Thus, the magnetic field mixes spins and the $+z$ or $-z$ polarized states are no longer eigenstates in the channel. Equations (8) also show that the spin quantization (eigenspinor) in any subband is not fixed and strongly depends on the wave vector k_x. Thus, an electron entering the semiconductor channel from the left ferromagnetic contact with $+x$-polarized spin, will not couple *equally* to $+z$ and $-z$ states. The relative coupling will depend on the electron's energy. This has a harmful effect on spin interferometers which will be discussed elsewhere.

B. Ferromagnetic contacts

We model the ferromagnetic contacts by the Stoner-Wohlfarth model. The magnetization of the contacts are assumed to be along the x-direction so that the majority carriers are $+x$-polarized electrons (as in Ref. 1) and minority carriers are $-x$-polarized. Their bands are offset by an exchange splitting energy Δ (Fig. 2).

IV. TRANSMISSION THROUGH THE INTERFEROMETER

Next, we calculate the total transmission coefficient through the spin interferometer for an electron entering from the left ferromagnetic contact (region I) and exiting at the right ferromagnetic contact (region III). A rigorous treatment of this problem would require an accurate modeling of the three- to one-dimensional transition between the bulk ferromagnetic contacts (regions I and III) and the quantum wire semiconductor channel (region II).[9,10] However, a one-dimensional transport model to calculate the transmission coefficient through the structure is known to be a very good approximation when the Fermi wave number in the ferromagnetic contacts is much larger than the inverse of the transverse dimensions of the quantum wire.[11,12] This is always the case with metallic contacts.

In region II ($0<x<L$), the x-component of the wave function at a position x along the channel is given by

$$\psi_{\rm II}(x)=A_{\rm I}\begin{bmatrix}C_1(k_{x,1})\\C_1'(k_{x,1})\end{bmatrix}e^{ik_{x,1}x}+A_{\rm II}\begin{bmatrix}C_1(-k_{x,1})\\C_1'(-k_{x,1})\end{bmatrix}e^{-ik_{x,1}x}+A_{\rm III}\begin{bmatrix}C_2(k_{x,2})\\C_2'(k_{x,2})\end{bmatrix}e^{ik_{x,2}x}+A_{\rm IV}\begin{bmatrix}C_2(-k_{x,2})\\C_2'(-k_{x,2})\end{bmatrix}e^{-ik_{x,2}x}. \quad (10)$$

For a $+x$-polarized electron in the left ferromagnetic contact (region I; $x<0$), the electron is spin polarized in the $[1,1]^\dagger$ subband and the x-component of the wave function is given by

$$\psi_{\rm I}(x)=\frac{1}{\sqrt{2}}\begin{bmatrix}1\\1\end{bmatrix}e^{ik_x^ux}+\frac{R_1}{\sqrt{2}}\begin{bmatrix}1\\1\end{bmatrix}e^{-ik_x^ux}+\frac{R_2}{\sqrt{2}}\begin{bmatrix}1\\-1\end{bmatrix}e^{-ik_x^dx}, \quad (11)$$

where R_1 is the reflection amplitude into the $+x$-polarized band and R_2 is the reflection amplitude in the $-x$-polarized band.

In region III ($x>L$), the x-component of the wave function is given by

$$\psi_{\rm III}(x)=\frac{T_1}{\sqrt{2}}\begin{bmatrix}1\\1\end{bmatrix}e^{ik_x^u(x-L)}+\frac{T_2}{\sqrt{2}}\begin{bmatrix}1\\-1\end{bmatrix}e^{ik_x^d(x-L)}, \quad (12)$$

where T_1 and T_2 are the transmission amplitudes into the $+x$ and $-x$-polarized bands. The wave vectors

$$k_x^u=\frac{1}{\hbar}\sqrt{2m_0E}, \quad k_x^d=\frac{1}{\hbar}\sqrt{2m_0(E-\Delta)}, \quad (13)$$

are the x components of the wave vectors in the $+x$ and $-x$-polarized energy bands, respectively.

The eight unknowns $[R_1, R_2, T_1, T_2, A_i (i = \text{I,II,III,IV})]$ must be found by enforcing continuity of the wave function and the quantity $[1/m^*(x)](d\psi/dx + ik_R(x)\sigma_z\psi(x))$ at $x = 0$ and $x = L$. The latter condition insures continuity of the current density. This leads to a system of 8 coupled equations for the unknowns which must be solved to extract the transmission amplitudes T_1, T_2 in the $+x$ and $-x$-polarized energy bands in the right ferromagnetic contact.

V. CONDUCTANCE OF THE INTERFEROMETER

For the majority spin carriers in the ferromagnetic contact ($+x$-polarized spin), the linear response source-to-drain conductance of the spin interferometer at any temperature T is given by the Landauer formula,

$$G_{+x\text{-polarized}} = \frac{e^2}{4hkT}\int_0^\infty dE |T_{\text{tot}}(E)|^2 \,\text{sech}^2\left(\frac{E - E_F}{2kT}\right), \tag{14}$$

where

$$|T_{\text{tot}}(E)|^2 = |T_1(E)|^2 + (k_x^d/k_x^u)|T_2(E)|^2 \tag{15}$$

is the total transmission coefficient through the interferometer.

Similarly, the conductance of the minority spin carriers ($G_{-x\text{-polarized}}$) is calculated after repeating the scattering problem for electrons incident from the minority spin band in the contacts. Since the $+x$ and $-x$-polarized spin states are orthogonal in the contacts, the total conductance of the spin interferometer is then given by $G_{+x\text{-polarized}} + G_{-x\text{-polarized}}$.

VI. NUMERICAL EXAMPLES

We consider a spin interferometer consisting of a quasi-one-dimensional InAs channel between two ferromagnetic contacts. The electrostatic potential in the z-direction is assumed to be harmonic with $\hbar\omega = 10$ meV in Eq. (3). We also assume a Zeeman splitting energy of 0.34 meV, $g^* = 3$, and $m^* = 0.036 m_o$.[1] The Fermi level E_f and the exchange splitting energy Δ in the ferromagnetic contacts are 4.2 and 3.46 eV, respectively.[14]

The Rashba spin–orbit coupling strength α_R is typically derived from low-temperature magnetoresistance measurements.[13] To date, the largest reported experimental values of the Rashba spin–orbit coupling strength α_R has been found in InAs-based semiconductor heterojunctions. For a normal HEMT $In_{0.75}Al_{0.25}As/In_{0.75}Ga_{0.25}As$ heterojunction, Sato *et al.*[13] have reported variation of α_R from 30- to 15×10^{-12} eV m when the external gate voltage is swept from 0 to -6 V.

In the numerical results below, we calculated the conductance of a spin interferometer with a 0.2 μm long channel as a function of the gate voltage. Tuning the gate voltage varies the potential energy barrier ΔE_c. Therefore, we have effectively calculated the interferometer's conductance as a function of ΔE_c. In our calculations, we vary ΔE_c over a range of 10 meV which allows us to display several peaks of the Ramsauer oscillations for the selected separation between source and drain. The final energy ΔE_c is equal to the Fermi energy E_f. At that point, the Fermi energy lines up with the top of the potential barrier which corresponds to complete pinch-off of the channel when the carrier concentration falls to zero. Over that range of ΔE_c, we simulated several cases of Rashba spin–orbit coupling strength α_R variation with increasing ΔE_c (or increasing gate voltage): **Case 1**: α_R stays constant and is equal to the largest experimental value reported to date (30×10^{-12} eV m), **Case 2**: α_R varies linearly with ΔE_c from 30×10^{-12} eV m down to zero, and **Case 3**: α_R varies from zero to a maximum of 30×10^{-12} eV m, which is the reverse of the previous case. A situation where α_R actually increases with reduction of the carrier concentration in the channel was reported for inverted InAlAs/InGaAs heterostructures by Schapers *et al.*[15] Finally, we consider **Case 4** where α_R is varied from 3×10^{-10} eV m (a tenfold improvement over the largest reported experimental result) down to zero. This last case corresponds to a variation of the spin precession angle θ from about 10π to 0 over the range of ΔE_c considered.

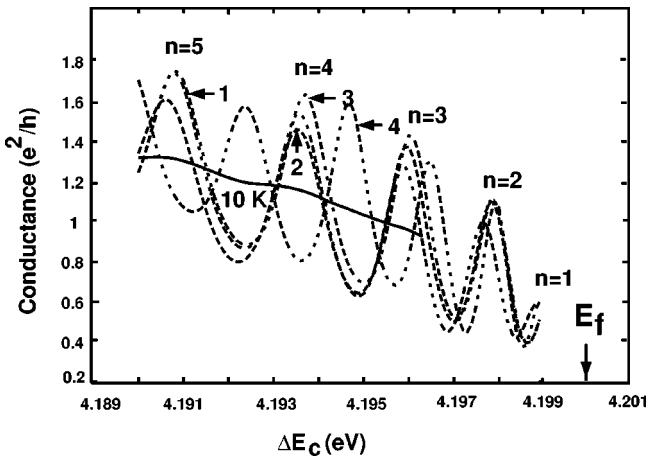

FIG. 3. Conductance modulation of the electron spin interferometer (for $T = 2$ K) for different variations of the Rashba spin–orbit coupling strength α_R with the energy barrier ΔE_c. The Fermi energy E_f is designated in the figure. The different α_R vs ΔE_c variations are labeled # 1 through #4 corresponding to cases 1 through 4 in the text. The separation between the two ferromagnetic contacts is 0.2 μm. The confinement energy $\hbar\omega$ is 10 meV. We have indicated the conductance peaks corresponding to different resonant energy levels (indexed by "*n*") lining up with the Fermi level in the contacts. The curve labeled $T = 10$ K represents the conductance modulation computed at a temperature of 10 K when α_R varies from 30×10^{-12} eV m to 0 as the gate voltage is varied.

The results of the conductance modulation are shown in Fig. 3 for the four cases described above at $T = 2$ K. This figure shows that there is very little change between the different curves corresponding to cases 1–3 of the α_R dependence on ΔE_c. The gate voltage variation of the Rashba spin splitting energy modifies slightly the shape and position of the resonant peaks due to electrostatic adjustment of the potential barrier between the two ferromagnetic contacts. Even for case 4, the amplitude of the conductance oscillations are

virtually unchanged and merely shifted along the ΔE_c axis compared to cases 1–3. Therefore, the Rashba effect only causes a weak modulation of the conductance oscillation due to the Ramsauer effect. In other words, the Ramsauer effect completely overshadows the Rashba effect.

The oscillations in conductance are more closely spaced as the quasi 1D channel approaches pinch-off. Consequently, the conductance modulation near pinch-off is more sensitive to temperature averaging. As illustrated in Fig. 3, the conductance oscillations are washed out completely for $T = 10$ K. We have shown this only for case 2 but similar degradation of the conductance modulation with temperature is found for all other cases considered here.

VII. CONCLUSION

In conclusion, we have shown that Ramsauer oscillations (or Fabry-Perot-type resonances) may be the dominant source of conductance modulation in 1D gate controlled electron spin interferometers. Thus, any experiment that purports to demonstrate the 1D spin interferometer needs to pay careful attention to the actual origin of the oscillations, lest the Ramsauer oscillations are mistaken for oscillations due to spin precession or Rashba effect. Since the Ramsauer oscillations are due to multiple reflections between the contacts of the interferometer, careful contact engineering is called for to eliminate these reflections. This may involve choosing an appropriate ferromagnet/semiconductor combination to reduce the potential barrier ΔE_c at the interface, while maintaining a high degree of spin polarization in the ferromagnet and a strong Rashba spin–orbit coupling in the semiconductor.

ACKNOWLEDGMENT

The work of S.B. was supported by the National Science Foundation under Grant No. ECS-0089893.

*Author to whom correspondence should be addressed. Email address: marc.cahay@uc.edu

[1] S. Datta and B. Das, Appl. Phys. Lett. **56**, 665 (1990).
[2] E.I. Rashba, Sov. Phys. Semicond. **2**, 1109 (1960); Y.A. Bychkov and E.I. Rashba, J. Phys. C **17**, 6039 (1984).
[3] This is a textbook example of one-dimensional tunneling problems. See for instance, H.C. Ohanian, *Principles of Quantum Mechanics* (Prentice–Hall, New Jersey, 1990), p. 96.
[4] T. Matsuyama, C.-M. Hu, D. Grundler, G. Meier, and U. Merkt, Phys. Rev. B **65**, 155322 (2002).
[5] J. Wróbel, T. Dietl, K. Fronc, A. Lusakowski, M. Czeczott, G. Grabecki, R. Hey, and K.H. Ploog, Physica E **10**, 91 (2001).
[6] A.V. Moroz and C.H.W. Barnes, Phys. Rev. B **60**, 14272 (1999); **61**, R2464 (2000).
[7] F. Mireles and G. Kirczenow, Phys. Rev. B **64**, 024426 (2001).
[8] M.H. Larsen, A.M. Lunde, and K. Flensberg, Phys. Rev. B **66**, 033304 (2002).
[9] A.M. Kriman and P.P. Ruden, Phys. Rev. B **32**, 8013 (1985).
[10] R. Frohne and S. Datta, J. Appl. Phys. **64**, 4086 (1988).
[11] D. Grundler, Phys. Rev. B **63**, 161307(R) (2001).
[12] O.E. Raichev and P. Debray, Phys. Rev. B **65**, 085319 (2002).
[13] J. Nitta, T. Akazaki, H. Takayanagi, and T. Enoki, Phys. Rev. Lett. **78**, 1335 (1997); G. Engels, J. Lange, Th. Schäpers, and H. Lüth, Phys. Rev. B **55**, 1958 (1997); Th. Schäpers, G. Engles, J. Lange, Th. Klocke, M. Hollfelder, and H. Lüth, J. Appl. Phys. **83**, 4324 (1998); C.-M. Hu, J. Nitta, T. Akazaki, H. Takayanagi, J. Osaka, P. Pfeffer, and W. Zawadzki, Phys. Rev. B **60**, 7736 (1999); J.P. Heida, B.J. van Wees, J.J. Kuipers, T.M. Kalpwijk, and G. Borghs, *ibid.* **57**, 11911 (1998); S. Brosig, K. Ensslin, R.J. Warburton, C. Nguyen, B. Brar, M. Thomas, and H. Kroemer, *ibid.* **60**, 13989 (1999); Th. Schäpers, J. Nitta, H.B. Heersche, and H. Takayanagi, *ibid.* **64**, 125314 (2001); Y. Sato, T. Kita, S. Gozu, and S. Yamada, J. Appl. Phys. **89**, 8017 (2001); Y. Sato, S. Gozu, T. Kita, and S. Yamada, Physica E **12**, 399 (2002).
[14] We use the same values as in F. Mireles and G. Kirczenow, Europhys. Lett. **59**, 107 (2002).
[15] Th. Schäpers, G. Engels, J. Lange, Th. Klocke, M. Hollfelder, and H. Luth, J. Appl. Phys. **83**, 4324 (1998).